M. BOZZI ZADRO, *et al.*
1968
N. 1 - *Supplemento* al *Nuovo Cimento*
Serie I. Vol. 6 - pag. 67-81

Spectral, Bispectral Analysis and Q of the Free Oscillations of the Earth.

M. BOZZI ZADRO
Istituto di Geodesia e Geofisica dell'Università - Trieste

M. CAPUTO
Istituto di Fisica dell'Università - Bologna

Introduction.

This paper analyses the records of the free oscillations of the Earth excited by the Chilean and the Alaskan earthquakes. The records for the Chilean earthquake were obtained with the pair of horizontal pendulums located in the Grotta Gigante near Trieste, and 4966 readings have been sampled at one-minute intervals for each record; the record of the Alaskan earthquake was obtained at the University of California, Los Angeles, with the LaCoste and Romberg gravity meter number 4, and 12 400 data have been sampled at one-minute intervals.

The aim of the investigation is to obtain the fine structure of the spectra, the specific dissipation of energy involved in the oscillations, and to study possible interactions of different modes due to nonlinear effects.

Wide use of spectral and bispectral analysis has been made; spectral methods based on the use of direct Fourier transforms have improved the results already obtained in previous investigations; the use of bispectral analysis has supplied evidence of interactions at the lowest frequencies.

1. – Fine structure of the energy spectra.

Before being processed, all the records have been filtered twice with an ideal high-pass filter with 201 values; the cut-off frequencies were selected at 1/6 cph for the records of the Chilean earthquake and at 3/20 cph for the record of the Alaskan earthquake.

As far as the Chilean earthquake records are concerned the total energy spectrum has been considered rather than the spectra of the individual records,

i.e. the spectrum of the energies associated with the ellipses of the horizontal ground displacement for each mode (1). The total energy spectrum is given by the sum of the squares of the semiaxes of the ellipses. The calculation of the semiaxes of the ellipses has been carried out using the direct Fourier transforms of the two records modulated with the von Hamming D_2 time window rather than the auto and cross correlation transforms, since the direct method allows a finer spectral resolution.

The elementary frequency band is of 4566^{-1} cpm; the computed frequencies have therefore a relative accuracy which is better than 10^{-2} for the lowest modes and better than 10^{-3} for the highest modes.

The spectrum is shown in Fig. 1.

The frequencies of the torsional and speroidal oscillations which have been identified are listed in Table I.

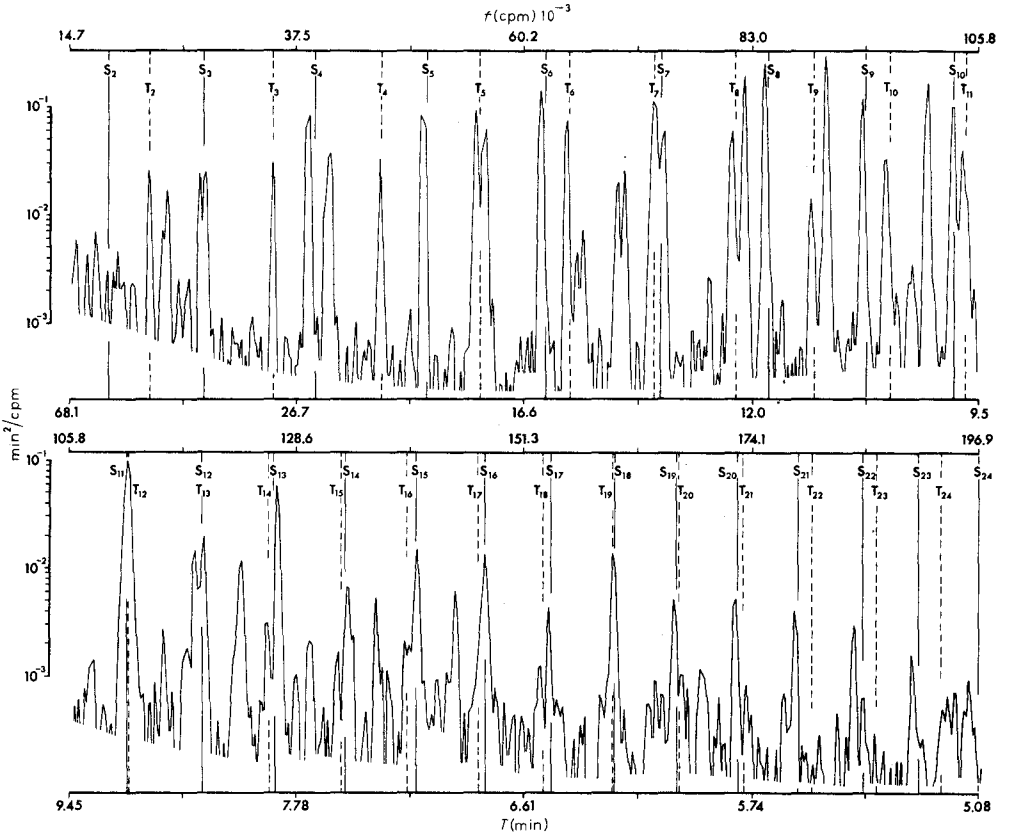

Fig. 1.

(1) M. BOZZI ZADRO and A. MARUSSI: *Geophys. Journ. Roy. Astr. Soc.*, **12**, 425 (1967).

TABLE I. – *Theoretical (Bullen B and Gutenberg) and observed periods of the free oscillations of the Earth (in minutes).*

Modes	Theoretical Gutenberg	Theoretical Bullen *B*	Chilean 4566 data	Δt	Alaskan 12000 data	Δt
${}_0S_2$	53.52	53.70	54.36 52.48 51.30	± 0.31	55.56 54.80 53.22 52.41	± 0.12
${}_0T_2$	43.61	44.16	43.90	0.20		
${}_0S_3$	35.33	35.50	35.95 35.12	0.14	35.99 35.61 35.30	0.053
${}_0T_3$	28.23	28.60	28.36 27.84 27.51	0.088 0.080 0.076		
${}_0S_4$	25.54	25.73	25.65 25.23	0.071	25.87 25.73	0.028
${}_1S_2$	24.32	24.75	24.42	0.065	24.39 24.22	0.025
${}_0T_4$	21.62	21.91	21.74	0.052		
${}_0S_0$	20.72	20.65	20.85	0.048	20.85 20.46	0.018
${}_0S_5$	19.66	19.85	19.94	0.044	20.12 20.00 19.84 19.67	0.017
${}_0T_5$	17.84	18.07	17.98	0.035		
${}_1S_3$	17.63	17.94	17.63	0.034	17.66 17.52	0.013
${}_0S_6$	15.92	16.12	16.08	0.028	16.11 16.01	0.011

TABLE I (*continued*).

Modes	Theoretical Gutenberg	Theoretical Bullen *B*	Chilean 4566 data	Δt	Alaskan 12000 data	Δt
${}_0T_6$	15.36	15.54	15.43	$\pm$0.026		
${}_2S_2$	15.15	15.49	15.17	0.025	15.15 15.10	$\pm$0.0096
${}_1S_4$	14.11	14.38	14.27 14.14	0.022	14.29 14.10	0.0084
${}_0T_7$	13.57	13.72	13.59	0.020		
${}_0S_7$	13.44	13.64	13.39	0.020	13.45 13.39	0.0075
${}_2S_3$	13.25	13.58	13.20	0.019	13.34 13.28	0.0074
${}_0T_8$	12.22	12.33	12.27	0.017		
${}_1S_5$	12.05	12.32	12.08	0.016	12.08	0.0061
${}_0S_8$	11.74	11.95	11.80	0.015	11.89	0.0059
${}_0T_9$	11.15	11.23	11.19	0.014		
${}_2S_5$	10.92	11.12	11.00	0.013	11.10 10.98	0.0051
${}_0S_9$	10.54	10.77	10.57	0.012	10.79 10.68	0.0048
${}_0T_{10}$	10.28	10.34	10.31	0.012		
${}_1S_0$	10.00	10.01	10.06	0.011	10.22	0.0044
${}_3S_2$	9.67	9.78	9.905	0.011	9.977 9.915	0.0041
${}_0S_{10}$	9.65	9.88	9.674	0.010	9.683	0.0039
${}_0T_{11}$	9.55	9.59	9.573	0.010		
${}_0S_{11}$	8.95	9.18	8.935	0.0088	8.947	0.0033

TABLE I (*continued*).

Modes	Theoretical Gutenberg	Theoretical Bullen B	Chilean 4566 data	Δt	Alaskan 12 000 data	Δt
${}_0T_{12}$	8.93	8.95		± 0.0088	8.927	± 0.0033
${}_0T_{13}$	8.39	8.40	8.424	0.0078		
${}_0S_{12}$	8.38	8.61	8.363	0.0077	8.375	0.0029
${}_4S_2$	7.98	7.99	8.110	0.0072	8.044 7.999	0.0027
${}_0T_{14}$	7.93	7.92	7.941	0.0069	7.896 7.849	0.0026
${}_0S_{13}$	7.90	8.11	7.886	0.0068		
${}_0T_{15}$	7.51	7.50	7.522	0.0062		
${}_0S_{14}$	7.48	7.68	7.473	0.0061	7.475	0.0023
${}_0T_{16}$	7.15	7.12	7.168 7.146	0.0056		
${}_0S_{15}$	7.11	7.30	7.101	0.0055	7.129 7.110	0.0021
${}_0T_{17}$	6.81	6.78	6.774	0.0050		
${}_0S_{16}$	6.78	6.96	6.774	0.0050		
${}_0T_{18}$	6.52	6.48	6.532	0.0047		
${}_0S_{17}$	6.49	6.66	6.495	0.0046		
${}_0T_{19}$	6.24	6.20	6.238	0.0043		
${}_0S_{18}$	6.23	6.39	6.238	0.0043		
${}_0S_{20}$	5.78	5.91	5.794	0.0037		
${}_0T_{21}$	5.77	5.72	5.794	0.0037		
${}_0S_{21}$	5.59	5.70	5.602	0.0034		

The power spectrum for the Alaskan record has been also computed using the direct Fourier transform of the data modulated with the von Hamming D_2 time window. The power spectrum is given by the squared modulus of the Fourier transform of the time series.

Indicating by $X(f)$ the complex Fourier transform of the time series $x(t)$ and by $Q_2(f)$ the transform of the $D_2(t)$ window, the apparent power spectrum obtained by using the direct Fourier transform is given by

$$|X(f) * Q_2(f)|^2, \tag{1.1}$$

whereas the use of the autocorrelation method supplies the spectrum in the form

$$|X(f)|^2 * Q_2(f) . \tag{1.2}$$

In the simplified case of a line spectrum with conveniently spaced lines the spectrum is given approximately by

$$|X(f) * Q_2(f)|^2 \simeq |X(f)|^2 * |Q_2(f)|^2 . \tag{1.3}$$

The weighting function being the square of the $Q_2(f)$ spectral window results in a narrower window than in the case of the autocorrelation method.

The periods of the identified spheroidal modes are listed in the Table I; the elementary frequency band is here $(12\,000)^{-1}$ cpm; the relative accuracy of the computed frequencies is therefore better than $2 \cdot 10^{-3}$ for the lowest modes, and better than $2 \cdot 10^{-4}$ for the highest modes.

The same Table I shows also the frequencies computed according to model Guntenberg Bullen *A* and model Gutenberg Bullen *B*. No correction has been applied to take into account the effects of the flattening of the Earth (2).

As can be seen, in both analyses the fundamental modes up to the 15th order (in the Chilean data analysis up to the 18th order), the first overtones and also some of the multiplets originated by the rotation of the Earth have been identified.

The observed frequencies are generally larger than those of the Gutenberg Bullen *B* model and smaller than those of Gutenberg Bullen *A* model, and closer to the Bullen *A* model.

2. – Dissipation of energy (Chilean earthquake data).

Each record of the Chilean earthquarke has been subdivided into five subsequent sections of 2700 data points. Each section lags 466 minutes with respect to the preceding one.

(2) M. CAPUTO: *Journ. Geophys. Res.*, **68**, 497 (1963).

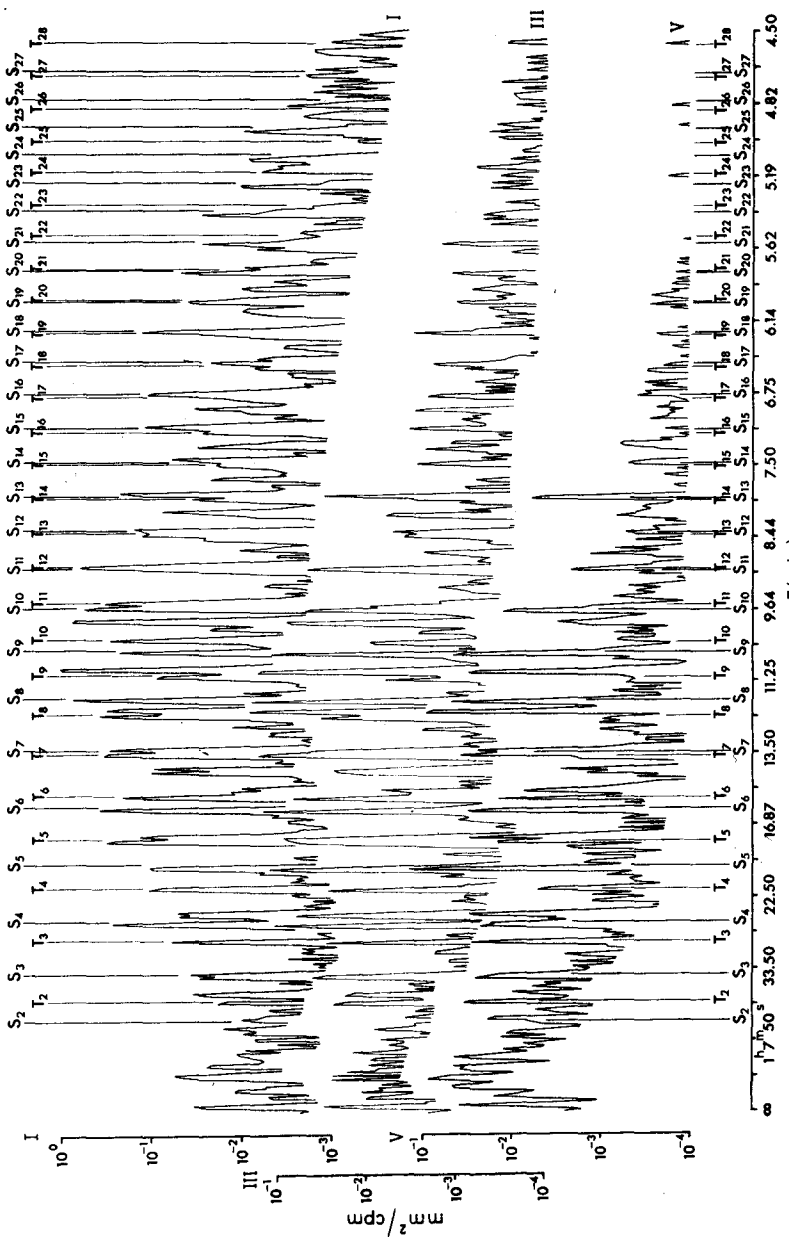
I
III
V
mm²/cpm
T (min)
1h 7m 50s
33.50
22.50
16.87
13.50
11.25
9.64
8.44
7.50
6.75
6.14
5.62
5.19
4.82
4.50

Fig. 2.

TABLE II *a*). – *Q*, Q^{-1} *and mean* Q^{-1} *values obtained for the torsional oscillations.*

	${}_0T_3$		${}_0T_9$	
	Q	Q^{-1}	Q	Q^{-1}
I/II	251	$3.98 \cdot 10^{-3}$	173	$5.78 \cdot 10^{-3}$
II/III	311	$3.22 \cdot 10^{-3}$	188	$5.32 \cdot 10^{-3}$
III/IV	610	$1.64 \cdot 10^{-3}$	181	$5.53 \cdot 10^{-3}$
I/III	278	$3.60 \cdot 10^{-3}$	181	$5.53 \cdot 10^{-3}$
II/IV	411	$2.43 \cdot 10^{-3}$	185	$5.41 \cdot 10^{-3}$
Q_M^{-1}		$2.97 \cdot 10^{-3}$		$5.51 \cdot 10^{-3}$
	${}_0T_4$		${}_0T_{10}$	
	Q	Q^{-1}	Q	Q^{-1}
I/II	199	$5.03 \cdot 10^{-3}$	170	$5.88 \cdot 10^{-3}$
II/III	166	$6.02 \cdot 10^{-3}$	160	$6.25 \cdot 10^{-3}$
III/IV	178	$5.62 \cdot 10^{-3}$	146	$6.85 \cdot 10^{-3}$
I/III	181	$5.52 \cdot 10^{-3}$	165	$6.06 \cdot 10^{-3}$
II/IV	172	$5.81 \cdot 10^{-3}$	153	$6.54 \cdot 10^{-3}$
Q_M^{-1}		$5.60 \cdot 10^{-3}$		$6.32 \cdot 10^{-3}$
	${}_0T_6$		${}_0T_{11}$	
	Q	Q^{-1}	Q	Q^{-1}
I/II	368	$2.72 \cdot 10^{-3}$	176	$5.68 \cdot 10^{-3}$
II/III	285	$3.51 \cdot 10^{-3}$	169	$5.92 \cdot 10^{-3}$
III/IV	278	$3.60 \cdot 10^{-3}$	276	$3.62 \cdot 10^{-3}$
I/III	321	$3.12 \cdot 10^{-3}$	173	$5.78 \cdot 10^{-3}$
II/IV	282	$3.55 \cdot 10^{-3}$	210	$4.76 \cdot 10^{-3}$
Q_M^{-1}		$3.30 \cdot 10^{-3}$		$5.15 \cdot 10^{-3}$
	${}_0T_8$			
	Q	Q^{-1}		
I/II	192	$5.21 \cdot 10^{-3}$		
II/III	183	$5.46 \cdot 10^{-3}$		
III/IV	130	$7.69 \cdot 10^{-3}$		
I/III	187	$5.35 \cdot 10^{-3}$		
II/IV	152	$6.58 \cdot 10^{-3}$		
Q_M^{-1}		$6.06 \cdot 10^{-3}$		

TABLE II *b*). – Q, Q^{-1} *and mean* Q^{-1} *values obtained for the spheroidal oscillations.*

	${}_0S_6$		${}_0S_{11}$	
	Q	Q^{-1}	Q	Q^{-1}
I/II	462	$2.17 \cdot 10^{-3}$	307	$3.26 \cdot 10^{-3}$
II/III	277	$3.61 \cdot 10^{-3}$	205	$4.88 \cdot 10^{-3}$
III/IV	266	$4.43 \cdot 10^{-3}$	217	$4.61 \cdot 10^{-3}$
I/III	346	$2.89 \cdot 10^{-3}$	246	$4.07 \cdot 10^{-3}$
II/IV	249	$4.02 \cdot 10^{-3}$	211	$4.74 \cdot 10^{-3}$
Q_M^{-1}		$3.41 \cdot 10^{-3}$		$4.31 \cdot 10^{-3}$
	${}_0S_8$		${}_2S_5$	
	Q	Q^{-1}	Q	Q^{-1}
I/II	359	$2.79 \cdot 10^{-3}$	297	$3.37 \cdot 10^{-3}$
II/III	354	$2.83 \cdot 10^{-3}$	280	$3.57 \cdot 10^{-3}$
III/IV	379	$2.64 \cdot 10^{-3}$	267	$3.75 \cdot 10^{-3}$
I/III	356	$2.81 \cdot 10^{-3}$	288	$3.47 \cdot 10^{-3}$
II/IV	366	$2.73 \cdot 10^{-3}$	273	$3.66 \cdot 10^{-3}$
Q_M^{-1}		$2.76 \cdot 10^{-3}$		$3.56 \cdot 10^{-3}$
	${}_0S_{10}$		${}_3S_2$	
	Q	Q^{-1}	Q	Q^{-1}
I/II	236	$4.24 \cdot 10^{-3}$	287	$3.48 \cdot 10^{-3}$
II/III	279	$3.58 \cdot 10^{-3}$	210	$4.76 \cdot 10^{-3}$
III/IV	414	$2.42 \cdot 10^{-3}$	196	$5.10 \cdot 10^{-3}$
I/III	256	$3.91 \cdot 10^{-3}$	243	$4.12 \cdot 10^{-3}$
II/IV	333	$3.00 \cdot 10^{-3}$	203	$4.93 \cdot 10^{-3}$
Q_M^{-1}		$3.43 \cdot 10^{-3}$		$4.48 \cdot 10^{-3}$

The Fourier transforms of all the sections and for both components, have been computed. The inspection of the amplitude and phase spectra obtained proves, as already seen in the past (1), that the horizontal oscillations are polarized and that the polarization of a mode changes in time. As a consequence the transfer of energies between the two components with time would influence the determination of the Q factor if computed from the successive energy spectra of the two components separately.

For this reason, the Q factors have been computed comparing the total

energy spectra of the five sections (see Fig. 2), thus suppressing the effect of the polarization changes.

Whereas in the former analysis very large bands of frequency were used to obtain average values of Q ([3]), in the present analysis the Q factor has been obtained, thanks to the fine structure of the spectra, for individual peaks, *i.e.* for 7 torsional and 6 spheroidal modes, selected from the strongest ones of sure attribution.

The frequencies and the energies used for the determination of Q have been computed by parabolic interpolation between three successive spectral values.

The last section has been disregarded owing to the high noise-to-signal ratio.

The Q and Q^{-1} obtained by considering the sections I and II, II and III III and IV, I and III, II and IV, as well as the mean Q^{-1} values are listed in Tables II *a*) and II *b*).

3. – Bispectral analysis.

Both in the spectra of the Chilean and Alaskan earthquakes several remarkable peaks are present which do not correspond to any theoretical frequency. These peaks may arise from the interaction of different modes as a consequence of nonlinear phenomena, in which case the associated frequencies are expected to be the sum or the difference of normal frequencies. In order to check if this hypothesis is acceptable, the bispectral analysis of the first 2700 minutes of the EW pendulum record of the Chilean earthquake has been carried out by using the direct Fourier transform method.

If $x(t)$ indicates the time series and $X(f)$ its Fourier transform (in general a complex function), the bispectrum is given by the ensemble mean

$$\langle X(f_1)\, X(f_2)\, X^*(f_3)\rangle \,, \tag{3.1}$$

where $f_3 = f_1 + f_2$ ([4]).

Assuming $X(f) \neq 0$ for $f_1 = \bar{f}_1$ and $f_2 = \bar{f}_2$, the ensemble mean in (3.1) is different from 0 for $f_1 = \bar{f}_1$, $f_2 = \bar{f}_2$, only if $X^*(\bar{f}_1 + \bar{f}_2) \neq 0$.

The physical significance of the bispectrum is easily seen by considering

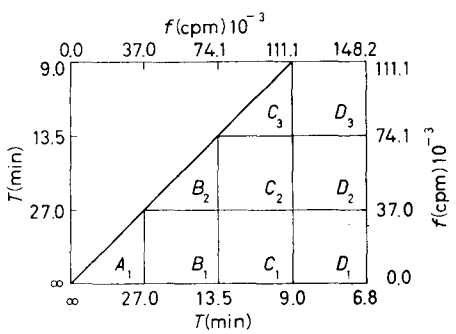

Fig. 3.

([3]) A. MARUSSI: *Rend. Accad. Naz. Lincei, Cl. Sc. Fis. Mat. Nat.*, Serie VIII, vol. **42**, fasc. I (1966).

([4]) K. HASSELMANN, W. MUNK and G. MACDONALD: *Bispectra of ocean waves*, in *Proceedings of the Symposium on Time Series Analysis*, ed. M. ROSENBLATT (New York, London, 1962).

that whereas the spectrum $\langle X(f_1)X^*(f_2)\rangle$ represents the contribution to the mean square $\langle x^2(t)\rangle$ arising from two frequencies $\bar{f}_1, \bar{f}_2$ such that $\bar{f}_1 + \bar{f}_2 = 0$, the bispectrum given by (3.1) represents the contribution to the mean $\langle x^3(t)\rangle$ arising from the frequencies $\bar{f}_1, \bar{f}_2, \bar{f}_3$ such that $\bar{f}_1 + \bar{f}_2 + \bar{f}_3 = 0$.

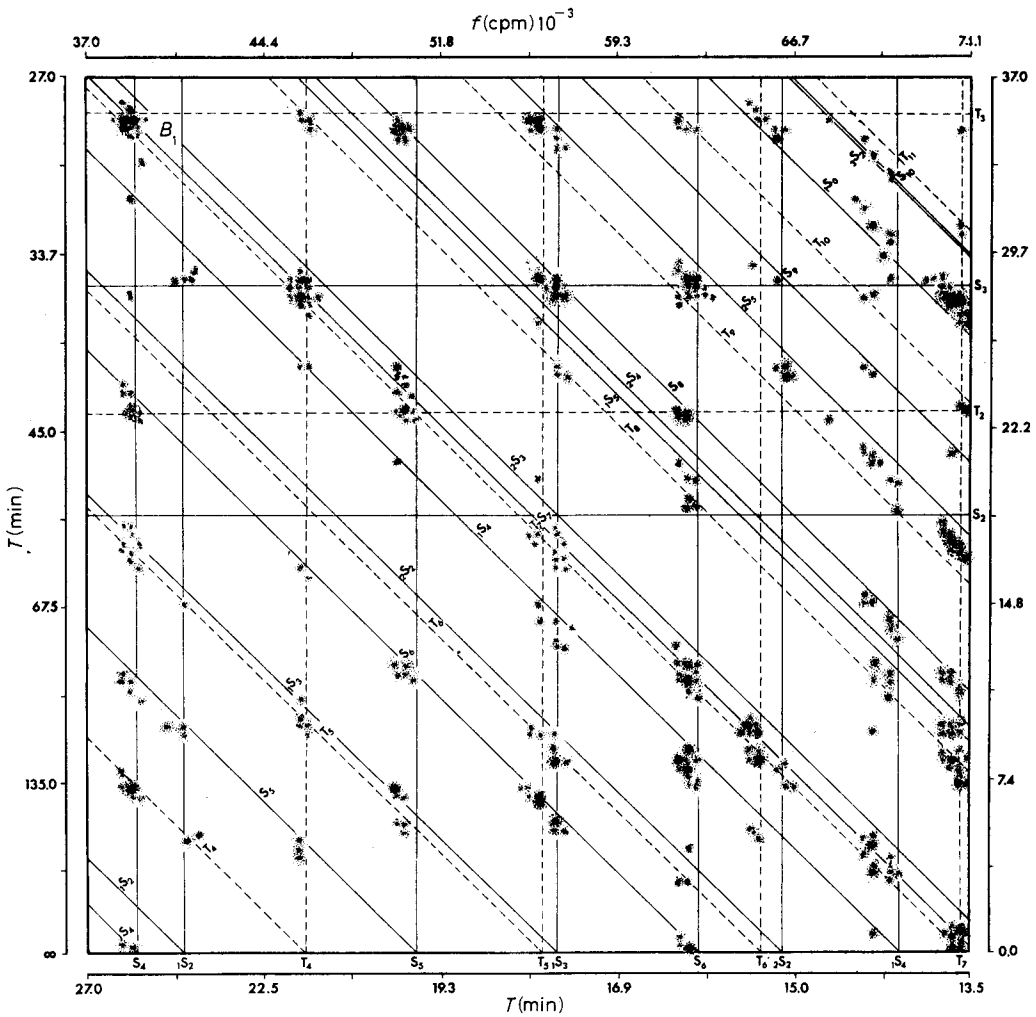

Fig. 4*a*.

The bispectral values have been computed only for the positive frequencies $f_2 \leqslant f_1 < 0.150$ cpm; the frequencies $f_2 > f_1$ have not been considered for reasons of symmetry, and the frequencies $f_1 > 0.150$ cpm have also not been considered since significant bispectral peaks do not appear beyond the frequency $f_1 = 0.11000$ cpm.

The modulus of the bispectrum has been represented in the form of a density distribution on a grid of squares on the plane $(f_1 f_2)$ as indicated in Fig. 3. As an example we give in Fig. 4 and 5 the maps concerning the squares indi-

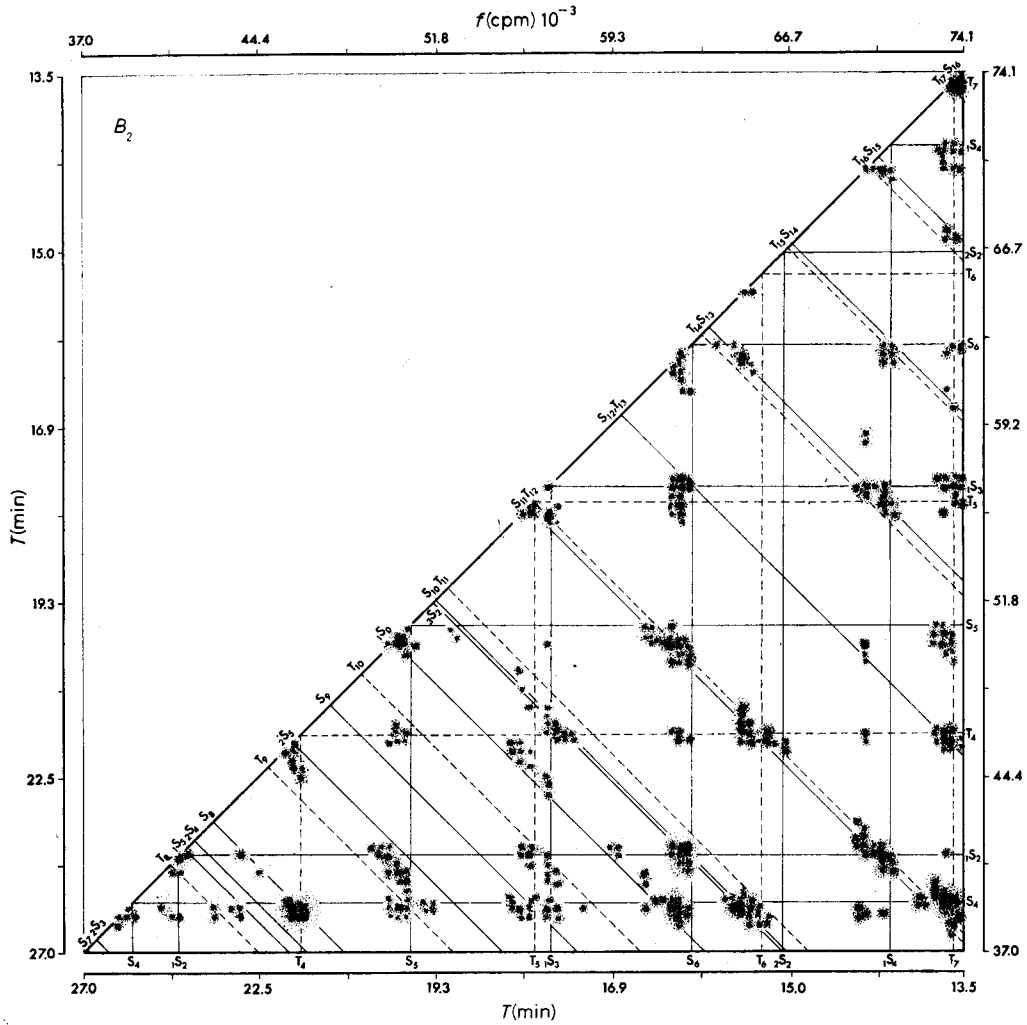

Fig. 4*b*.

cated by B_1, B_2, C_1 and C_2 showing the observed bispectral density and the lines corresponding to the theoretical values of the normal modes. The bispectral density maxima for which all three frequencies involved are normal modes are not significant.

This case is most common at the higher frequencies f_1 and f_2 (B_2, C_2, C_3 squares) where the combination $\pm f_1 \pm \bar{f}_2$ of the frequencies of two normal modes, $\bar{f}_1$ and $\bar{f}_2$, is very often close to the frequency of another normal mode,

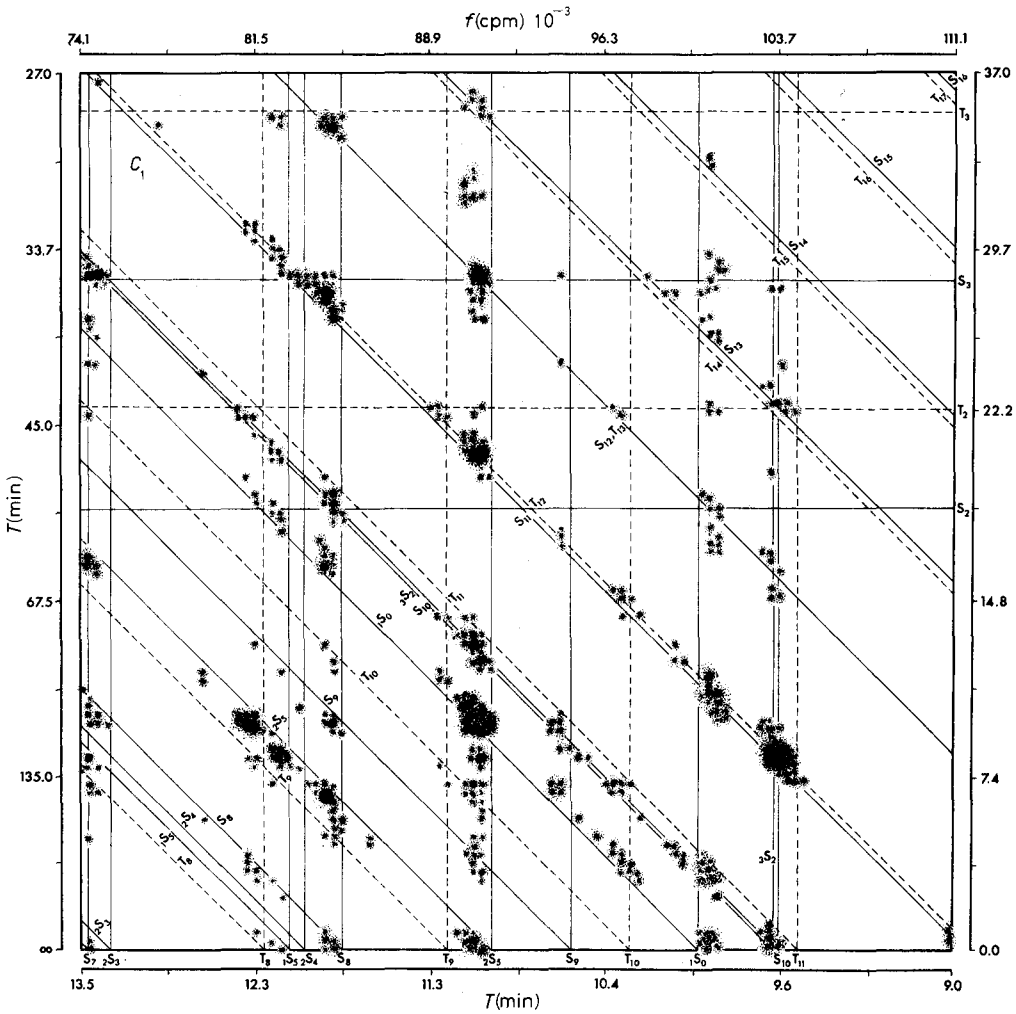

Fig. 5*a*.

the broadening of the bispectral peaks due to the time window and to the dissipation being the major factor of uncertainty in the identification.

Some bispectral maxima are associated with the frequencies of two known modes $\bar{f}_1$ and $\bar{f}_2$ while the third frequency $f_3 = \pm \bar{f}_1 \pm \bar{f}_2$ is not; in this case

f_3 is tentatively attributed to nonlinear effects. This is the case for the bispectral maxima present in the strip limited by the frequencies $f_2 = 0.0$ cpm and $f_2 = 0.040$ cpm.

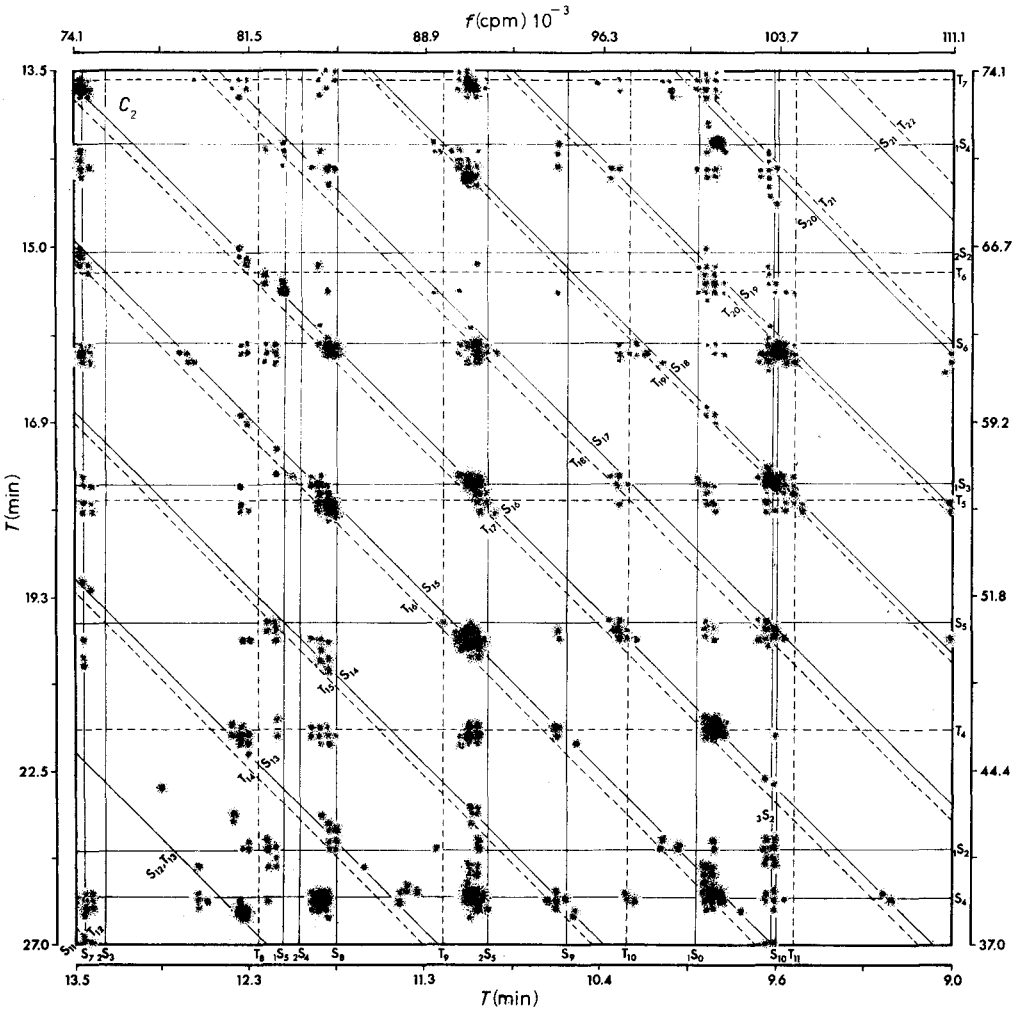

Fig. 5*b*.

In Table III the most important interacting modes as well as the periods observed in the bispectrum and in Chilean and Alaskan spectra are listed.

The interaction seems to be almost absent between the modes up to ${}_0S_4$ as well as between the modes beyond ${}_0S_{11}$.

TABLE III.

Interaction modes	Observed periods in bispectrum (min)	Observed periods Chilean 4566 data spectrum (min)	Observed periods Alaskan 12000 data spectrum (min)
${}_0S_8 - {}_2S_5$	150	152	149
${}_0S_4 - {}_0T_4$	142	143	143
${}_0T_8 - {}_2S_5$	104	106	103
${}_2S_5 - {}_1S_0$	104	106	103
${}_2S_5 - {}_0S_{10}$	79	79	79 80
${}_0S_8 - {}_1S_0$	61	61	61
${}_2S_5 - {}_0S_{11}$	47	48	47 48

The greatest bispectral maxima partially supported by spheroidal modes between ${}_0S_6$ and ${}_0S_{10}$ in particular the ${}_2S_5$ mode interacts consistently with almost all the modes whose frequency is near to its own frequency.

* * *

This research has been supported partially by E.R.O., U.S. Army, under contract DA-91-591-3960, and C.N.R., under contract n. 115.0201.0.